Mobilization of coarse surface layers in gravel-bedded rivers by finer gravel bed load

J. G. Venditti,[1] W. E. Dietrich,[2] P. A. Nelson,[2] M. A. Wydzga,[3] J. Fadde,[4,5] and L. Sklar[4]

Received 25 June 2009; revised 25 January 2010; accepted 15 February 2010; published 10 July 2010.

[1] Additions of sand to gravel beds greatly increase the mobility and flux of gravel. However, it is not known how additions of finer gravel to coarser gravel beds will affect the mobility of bed material. Here we examine the effect of fine gravel pulses on gravel bed material transport and near-bed flow dynamics in a series of flume experiments. Bed material refers exclusively to sediment in the channel prior to the pulse introduction. The observations indicate that fine sediment pulses tend to migrate downstream in low-amplitude waves. As the waves pass over the gravel bed, the interstitial pockets in the bed material surface fill and coarse gravel particles are entrained. This increases bed material transport rates and causes a distinct shift from a selective mobility transport regime where particles coarser than the bed material median (8 mm) make up <30% of the load to an equal mobility transport regime where bed materials coarser than 8 mm and finer than 8 mm are transported in equal proportions. The only possible source for this coarser bed load material is the sediment bed, suggesting that portions of the coarse surface layer are being mobilized. Observations of near-bed velocity and turbulence suggest that fine gravel pulses cause fluid acceleration in the near-bed region associated with a reduction in the level of turbulence produced at the sediment boundary. This accelerated fluid at the bed increases drag exerted on coarse surface layer particles, promoting their mobilization. Our findings suggest that, in general, finer bed sediment (not just sand) can mobilize coarser sediment and that expressions for the influence of sand on bed mobility need to be generalized on the basis of grain ratios.

Citation: Venditti, J. G., W. E. Dietrich, P. A. Nelson, M. A. Wydzga, J. Fadde, and L. Sklar (2010), Mobilization of coarse surface layers in gravel-bedded rivers by finer gravel bed load, *Water Resour. Res.*, *46*, W07506, doi:10.1029/2009WR008329.

1. Introduction

[2] It is well established that additions of sand to a gravel bed will increase gravel transport rates in river channels [*Jackson and Beschta*, 1984; *Iseya and Ikeda*, 1987; *Wilcock and McArdell*, 1993, 1997; *Wilcock*, 1998; *Wilcock et al.*, 2001; *Wilcock and Kenworthy*, 2002; *Curran and Wilcock*, 2005], effectively mobilizing the bed surface. The exact mechanisms are not well understood, but the change can be represented by changes in the critical value of the Shields number (τ_*) for entrainment of gravel:

$$\tau_* \equiv \frac{\tau_b}{(\rho_s - \rho_w)gD}, \tag{1}$$

where τ_b is the shear stress at the bed; D is the diameter of a particle and is usually taken as the surface median size for beds of mixed grain size; ρ_s and ρ_w are the densities of the sediment and fluid, respectively; and g is gravitational acceleration. *Wilcock* [1998] and *Wilcock and Kenworthy* [2002] demonstrate that there is a reduction of the critical value of τ_* for entrainment by about a factor of 3.5 as the percent of the bed area covered with sand increases. This reduces τ_* by about 2 times as sand converge increases in the empirical model of *Wilcock and Crowe* [2003] because some of the effects of the fines is implicit in a hiding function (which represents the sheltering of smaller grains by larger particles) and differences in median surface grain size between sand-rich and sand-poor surfaces.

[3] *Ikeda* [1984] first proposed a mechanism for the increased mobility of gravel with an addition of sand, indicating that it is due to some combination of (1) hydraulic smoothing of the bed by sand, which reduces the drag of surface gravel particles and increases near-bed flow velocity; (2) reductions in the friction angle (the pivot angle a particle must rotate over to be entrained into transport); and (3) a lack of "disentrainment" locations on the bed surface (where particles can be caught in the wakes of a protruding particles). A number of authors have expanded upon this early work, using the proposed mechanisms to explain bed load sheet formation [*Whiting et al.*, 1988] and the restriction of active sediment transport zones in response to reduced sediment supply [*Dietrich et al.*, 1989]. For example, *Whiting et al.* [1988] note that the mobility of the various

[1]Department of Geography, Simon Fraser University, Burnaby, British Columbia, Canada.
[2]Department of Earth and Planetary Science, University of California, Berkeley, California, USA.
[3]Department of Earth Science, University of California, Santa Barbara, California, USA.
[4]Department of Geosciences, San Francisco State University, San Francisco, California, USA.
[5]Stillwater Sciences, Berkeley, California, USA.

0043-1397/10/2009WR008329

fractions that compose a mixed-size sediment is controlled by the pocket geometry within which grains rest and the size of grains that compose the surface layer. They hypothesize that as pockets fill with finer sediment, there is a reduction in the momentum loss caused by wake formation on particles projecting into the flow, and those projecting particles experience increased drag as the near-bed flow velocity increases. *Whiting et al.* [1988] suggest that this process results in a grain-grain interaction whereby coarse particles are plucked from the bed by increased drag and coarse particles remain in motion because distrainment sites are filled with fine sediment. *Whiting et al.* [1988] proposed that the patchy nature of this infilling and the tendency for large grains to concentrate during the transport process could be responsible for bed load sheet formation. This roughness perturbation in the bed surface grain size has been linked to the growth of bed load sheets [*Seminara et al.*, 1996]. *Dietrich et al.* [1989] noted that when sediment supply to a channel is reduced, the availability of fine particles to infill pockets is reduced and the zone of active transport is restricted.

[4] *Kirchner et al.* [1990] and *Buffington et al.* [1992] further expanded on this work by examining the effects of the sediment size distributions on the friction angle that controls sediment entrainment. They demonstrated that as particles increase in size relative to the bed material surface, particle protrusion increases, which exposes greater proportions of large particles to the flow and projects the particle farther above the mean bed elevation. *Kirchner et al.* [1990] used a simple analytical model to demonstrate that increased particle projection increases the lift and drag forces on particles, increasing the likelihood of entrainment.

[5] In spite of our growing understanding of how sand additions to gravel beds affect sediment transport rates, direct measurements documenting the key linkages between near-bed velocity, pocket infilling with fine material, and large-grain mobilization have not been obtained. Also, it remains unknown whether gravel beds can be mobilized by additions of finer gravel by the same mechanisms as proposed for sand, although a number of authors have suggested this may be the case [cf. *Wilcock and Kenworthy*, 2002]. There is considerable interest in the problem from applied river scientists who seek to mobilize static river beds downstream from dams in an attempt to rejuvenate salmon spawning gravels. Gravel augmentation of finer gravel (without adding sand) may be able to unlock these beds.

[6] Here we conduct flume experiments to test the hypothesis that static coarse surface layers in gravel-bedded rivers can be mobilized through addition of suitably finer gravel bed load to the channel. We find that mobilization occurs and that local measures of velocity and turbulence support the mechanisms proposed by *Ikeda* [1984] and *Whiting et al.* [1988]. Our results imply that it is the grain ratio (and abundance of finer sediment), rather than simply sand abundance, that should be used in critical shear stress estimation and bed load transport calculations.

2. Experiments

[7] Experiments were conducted in a 28 m long and 0.86 m wide sediment feed flume at the Richmond Field Station, University of California, Berkeley. The sediment feed and initial bed stock were composed of a unimodal gravel with a median grain size D_{50} = 8 mm, a distribution truncated at 2 and 32 mm, and no sand present. Seven experimental runs were conducted during which finer gravel pulses were fed to an armored channel bed. In each case, the initial slope, the discharge, and the bed surface grain size distribution were the same. The experimental runs differed in the volume of the fine gravel pulse added to the channel, pulse grain size, the feed rate, and the frequency of pulse additions. Here we use data from two experimental runs to test our hypothesis.

[8] Discussion of the whole suite of experimental runs can be found in work by *Venditti et al.* [2010] and *Sklar et al.* [2009]. *Venditti et al.* [2010] report on the effects of sediment pulse grain size, volume, and frequency on bed mobility and fractional transport. *Sklar et al.* [2009] examine the translation and dispersion of sediment pulses in a channel without an upstream sediment supply.

[9] In reporting our experiments, we use the term bed material to refer to the initial bed stock used in our experiments. This sediment formed the subsurface in the flume. The term bed load is used to describe all material being transported in the channel and may include both the bed material and any pulse material that was introduced. Similarly, the bed surface is composed of the bed material and may include pulse material. The term bed material load is used to refer to material in transport that is sourced from the bed material and excludes pulse material.

[10] To discuss the effects of sediment additions, we need to distinguish between partial, selective, and equal mobility transport regimes. Here we follow the terminology of *Parker* [2007], where partial mobility transport is where the coarse tail of the bed load size distribution is finer than that of the bed surface. Selective mobility transport is where all sizes on the bed are found in the bed load but the bed load size distribution is finer than the bed surface. Equal mobility is where the bed load size distribution and the bed surface are the same [*Parker*, 2007]. Equal mobility of the bed load with respect to the subsurface sediment (rather than the surface) can occur in the presence of a coarse surface layer [e.g., *Parker and Klingeman*, 1982].

[11] Table 1 summarizes the pulse characteristics and hydraulics. Flows were fully turbulent in terms of the Reynolds number ($Re = h\overline{U}/\nu = 2.3 \times 10^5$, where h is flow depth, $\overline{U}$ is the mean velocity, and ν is kinematic viscosity) and hydraulically rough in terms of the grain Reynolds number ($Re_g = D_{50}u_*/\nu \approx 1500$, where u_* is the shear velocity) and lower regime in terms of the Froude number ($Fr = \overline{U}/\sqrt{gh} \approx 0.65$). The channel width-to-depth ratio of ~4 suppressed the development of lateral topography and allowed us to focus on grain-to-grain interactions.

[12] For each run, an equilibrium was first established between the sediment feed rate and sediment flux at the end of the channel. Sediment feed was then stopped and the flow was continued for >75 h at the same flow stage. This armored the channel until the bed surface medial size $D_{50surf} \approx 16$ mm and reduced the transport rate to 3%–6% of the original feed rate. We then added pulses of narrowly graded 3 mm gravel (D_{50} = 2.8 mm; Figure 1) that were painted to distinguish them from the bulk material in the flume. Pulses were added 5 m from the channel entrance at a feed rate (160 kg/h) that was ~4× the equilibrium bed load rate observed prior to terminating the sediment supply (40 kg/h). We used a number of pulse types, including

Table 1. Pulse Characteristics and Hydraulic Conditions for Select Fine Gravel Sediment Additions

	Pulse Characteristics				Hydraulic Conditions					
Run	Pulse Type	D_{50} (mm)	Volume (kg)	h (mm)	S[a]	U (m/s)	Fr	D_{50surf}[b] (mm)	D_{90surf}[b] (mm)	τ_*[c]
10	single addition	3	267.3	242	4×10^{-3}	0.99	0.64	16.3 (10.0)	23.8 (20.8)	0.035
21	multiple addition[d]	3	4 × 66.8	244	4×10^{-3}	0.98	0.63	16.5 (10.7)	24.8 (21.1)	0.036

[a]Slope is averaged over the entire flume.
[b]Based on area-by-weight physical samples of the bed surface. Numbers in parentheses have been converted to a volume-by-weight sample using the *Kellerhals and Bray* [1971] conversion.
[c]Sidewall corrected using the *Williams* [1970] method.
[d]Multiple pulses are a, b, c, and d, labeled in order of occurrence.

single small and large pulses as well as multiple pulses where four pulses were added to the channel with a short intervening period (labeled a, b, c, and d in order of occurrence; Table 1). Out of the seven pulse experiments completed, we focus here on runs 10 and 21, which were the large- and multiple-pulse runs, respectively.

[13] Run 10 produced the largest increase in sediment flux rate in the channel and thus had the greatest potential for significant mobilization. Because run 21 was composed of four pulses, each identical in size, we were able to focus on detailed observations of pulse progression and velocity during the individual pulses. This was not possible over single small pulses because the process happened so quickly that most of our effort was focused on synoptic observations of flow and pulse movements.

[14] During each run, we monitored pulse movement along the flume, the effect of pulse movement on bed and water surface topography, and bed load flux at the end of the flume and collected samples for bed load grain size analysis. During runs 21b and 21c, velocity at different heights above the centerline of the bed was recorded using two acoustic Doppler velocimeters, and we simultaneously tracked local bed and water surface height at a frequency of 1 or 2 Hz. We present data from the probe that were closer to the bed but also use the upper probe data to calculate the plane of zero velocity associated with the near-bed velocity profile. Bed load for all runs was monitored using a continuous weighing mechanism that recorded the weight of material leaving the flume at 60 s intervals [see *Venditti et al.*, 2010]. Periodically, the material in the collection mechanism was removed and sieved. In order to characterize the bed surface texture, at the end of each experimental run, a 0.2 × 0.2 m area of the bed surface was spray painted, each painted grain was removed, and the total collection of grains was sieved and weighed (to calculate the equivalent of a volume-by-weight sample, we followed the conversion procedure of *Kellerhals and Bray* [1971]).

3. Observations

3.1. Fine Gravel Pulse Morphodynamics

[15] Once introduced into the channel, the 3 mm pulses quickly translated downstream, growing in height. Figure 2 shows a time series of the change in the bed and water surface elevation along the flume collected during run 21d. Immediately following the pulse feed, the pulse sediment was entrained and moved downstream, reaching the flume exit after ~40 min. Fine sediment pulses formed and moved as low-amplitude, nearly symmetric migrating waves that, at their maximum thickness, covered the bed to a lateral extent ~3/4 of the width. The bed wave topography was uniform across the channel, tapering laterally at the edges. Between each bed wave, the coarser resident gravel was exposed. The thin upstream tail of the pulse moved downstream more quickly than the sediment-rich head.

[16] The velocity of the pulse head decreased as it moved downstream from 14.3 mm/s to 6.5 mm/s by the time it exited the flume. The difference in velocities of the head and tail of the pulse led to a shortening of the fine gravel pulse length and vertical thickening of the pulse from 10 mm during the feed (Figures 2a–2c) to 15 mm after the pulse feed ceased and the pulse moved into the last 10 m of the flume (Figures 2d–2g). As in other kinds of sediment waves, the increasing mass of the wave is accommodated by slowed migration [cf. *Venditti et al.*, 2005]. The topographic signature of the pulse was not obvious after 1 h (Figure 2g), but the pulse material remained present on the bed (Figure 2g), filling pockets between large particles for many hours following the pulse translation.

[17] After 7–8 h following the pulse introduction and no additional sediment feed, there was no significant difference in the bed surface texture compared to the prepulse condition (see *Sklar et al.* [2009] and *Venditti et al.* [2010] for further details). Indeed, there is no topographic signature of

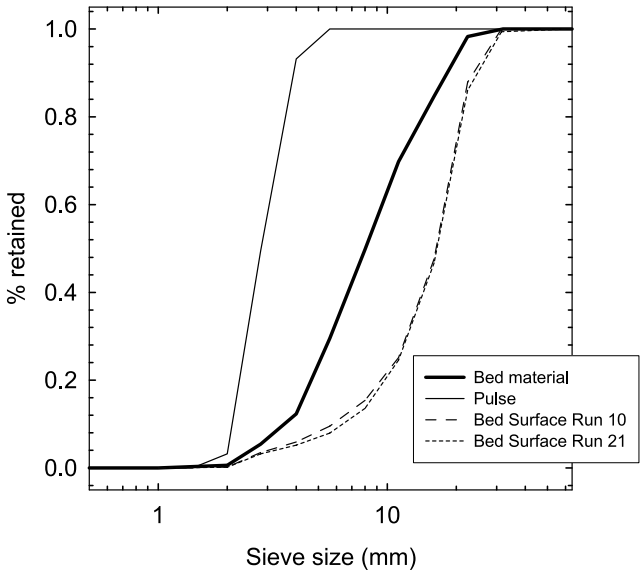

Figure 1. Grain size distribution of bed material and fine gravel pulse. The bed surface size distributions represent the armored surface and are weight-by-area samples.

the pulse on the bed. The difference profile after 7 h suggests that while the specific locations of topographic highs and lows have changed from the beginning of the experiment, the mean elevation was the same as the prepulse condition (Figure 2h).

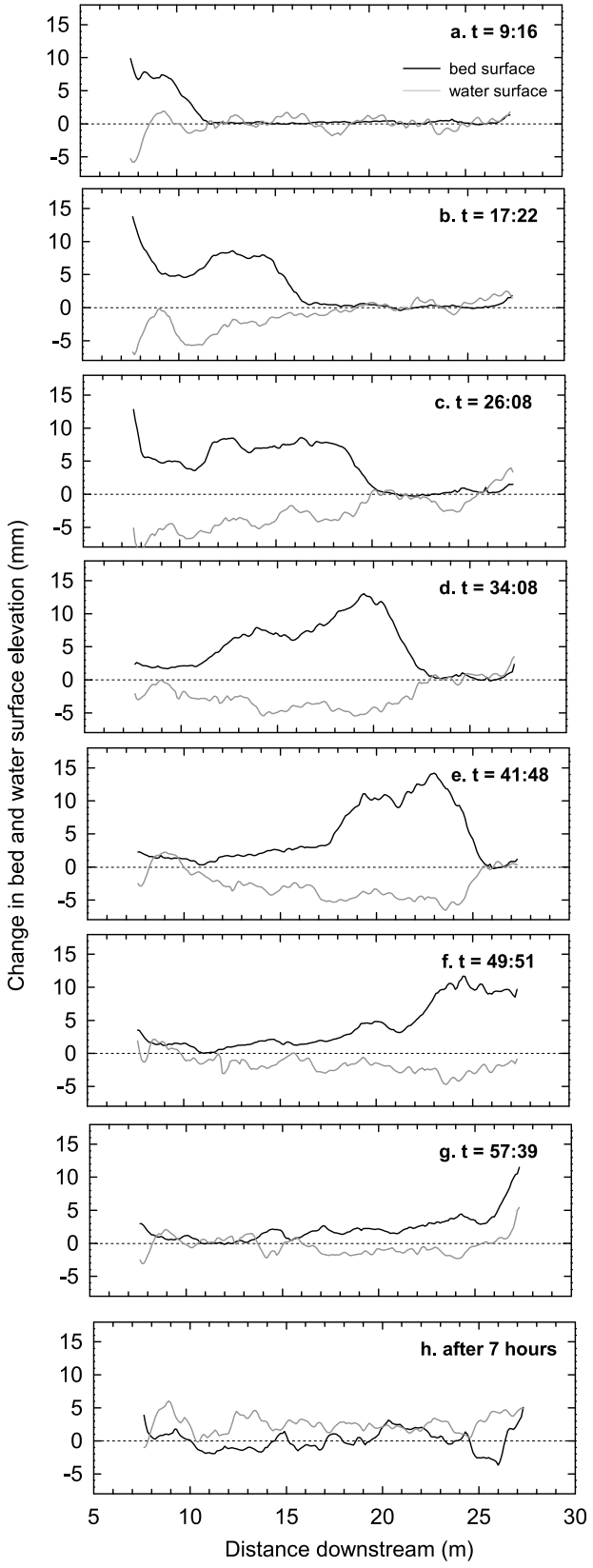

Figure 2. (a–h) Change in water surface and bed surface elevation along the flume. The elevation profiles measured at the times shown at the top right of each plot have been subtracted from the profiles measured at 100 s after the pulse feed began during run 21d. As such, the curves show the change in the water surface profile and the bed surface profile from the beginning of the experiment. The bed and water surface elevation were monitored using an ultrasonic water level sensor and an acoustic echo sounder built by the National Center for Earth Surface Dynamics and mounted on a movable cart that traversed the flume [see *Venditti et al.*, 2010]. For display purposes, these plots have been smoothed with a negative exponential algorithm that weights values using a Gaussian distribution and a bandwidth of 100 mm.

3.2. Bed Load Transport

[18] The sediment pulses rapidly migrated downstream, grew in height, and arrived with little dispersion at the downstream end (Figure 2). Figure 3 shows the observed bed load transport rate and the fraction of the bed load >8 mm and >11.2 mm in size as the pulse exited the flume during single large-pulse run 10. We chose reference values of 8 and 11.2 mm because they correspond to the sieve size closest to the bed material subsurface median (8.1 mm) and the weight-by-volume equivalent bed material surface median (10.0 for run 10 and 10.7 mm for run 21, Table 1).

[19] Prior to introducing the pulse to the channel during run 10, the bed was armored with the total sediment discharge rate, Q_s = 2.3 kg/h exiting the flume (equivalent to 0.04 mm/h lowering of the bed). As the main body of the pulse exited the flume, the average discharge rate rose to 159.3 kg/h, equivalent to the rate at which it was introduced to the channel. However, there were sustained periods when Q_s exceeded the input rate. After the main body of the pulse exited the channel, Q_s slowly declined from 30 kg/h back to the prepulse flux (~2 kg/h) at 12.5 h. The run was continued for an additional 18.3 h, which reduced the gravel flux to 1.1 kg/h.

[20] Integration of the Q_s curve in Figure 3a reveals that more material (330.1 kg) exited the channel than was fed upstream (267.0 kg). Given that 31% (82.7 kg) of the pulse went into storage in the channel, these values indicate a significant mobilization of coarser bed material (nonpainted particles). This is clear from an examination of the coarse fractions exiting the flume. At the beginning of run 10, the bed was in a selective transport regime [*Parker*, 2007] where the coarse fractions (>8 mm) of the bed material composed ~20% of the bed load and the finer fraction composed ~80% (Figure 3b). This selective mobility regime is a legacy effect of the previous fine sediment pulse introduced to the flume. Passage of the sediment pulse in the channel caused a shift to an equal mobility regime with respect to the subsurface where particles coarser than 8 mm composed ~50% of the bed load. As the main body of the pulse exited the flume, the fraction of coarse particles in the bed load declined, returning the flume to a selective transport regime similar to the initial condition.

[21] Figure 3b also shows that sediment coarser than the 11.2 mm grain size increased from 8% at the beginning of run 10 to ~20% while the pulse was in the channel and then returned to 10% after the pulse had exited the channel. The

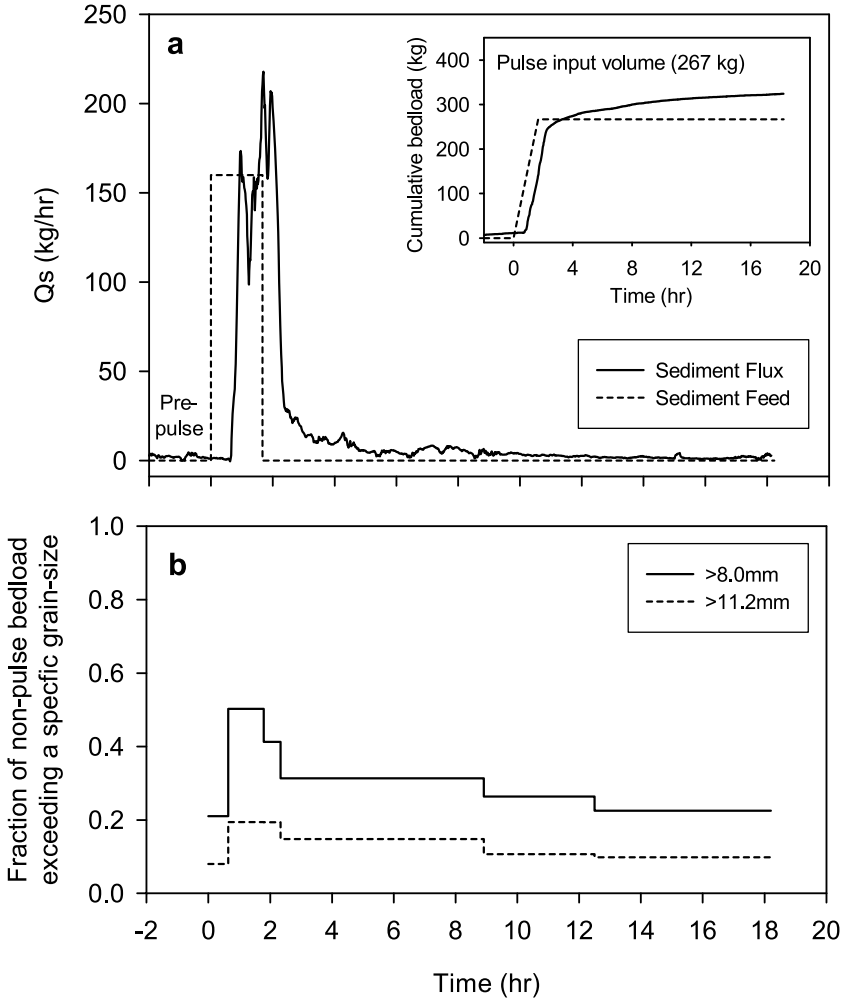

Figure 3. (a) Bed load transport and sediment feed during run 10. The sediment flux curve is a 600 s running average through a time series that was sampled at 60 s. (b) Fraction of the bed load composed of particles >8 mm and >11.2 mm. The values 8 and 11.2 mm correspond to the sieve size closest to the bed material subsurface median (8.1 mm) and the weight-by-volume equivalent bed surface median (10.0 for run 10 and 10.7 mm for run 21, Table 1).

increase in >11.2 mm material further suggests that the increase in fractional transport occurs by entrainment of the material making up the coarse surface layer.

3.3. Hydraulics and Smoothing

[22] The sediment pulses changed the local fluid flow structure and hydraulics as they migrated downstream. When the pulses passed beneath the instrument array, the water surface dropped 5.7 mm (Figure 4a). The drop was caused by both the rise in bed elevation and the smoothing effect of fine gravel. We attempted to quantify the importance of these two processes by calculating the velocity increase over the rise in the bed without accounting for the change in roughness. To do so, we use the 1-D conservation of energy (Bernoulli) equation written as

$$\overline{U}_2(t) = q_w \Big/ \left(h_1 + \frac{\left[\overline{U}_1{}^2 - \overline{U}_2(t)^2\right]}{2g} - z(t) \right), \qquad (2)$$

where t is time, h_1 and $\overline{U}_1$ are the flow depth and mean velocity prior to pulse passage, q_w is the specific water discharge (0.238 m^2/s in our experiments), and $\overline{U}_2$ is the velocity with a change in bed elevation z. Our initial values of h_1 and $\overline{U}_1$ are set by our measured values of flow depth (h) and flow velocity ($\overline{U}_m = q_w/h$) at the beginning of the experiment. The calculated velocity ($\overline{U}_2$) is solved for iteratively using the continuous record of $z(t)$. Equation (2) provides a velocity that will reflect a change in bed elevation but not a change in roughness because energy losses are neglected in this form of the energy equation. As such, the difference between our calculated values of $\overline{U}_2$ and our measured values are assumed to be due to changes in the bed roughness. Our calculation of $\overline{U}_2$ is conservative because we used the smoothed profiles displayed in Figure 4a.

[23] Figure 4b shows the changes in our measured mean velocity $\overline{U}_m$ and the calculated values of $\overline{U}_2$. As the pulse passed below the sensor array, $\overline{U}_m$ increased. There was greater variation in $\overline{U}_m$ when the pulse was passing below

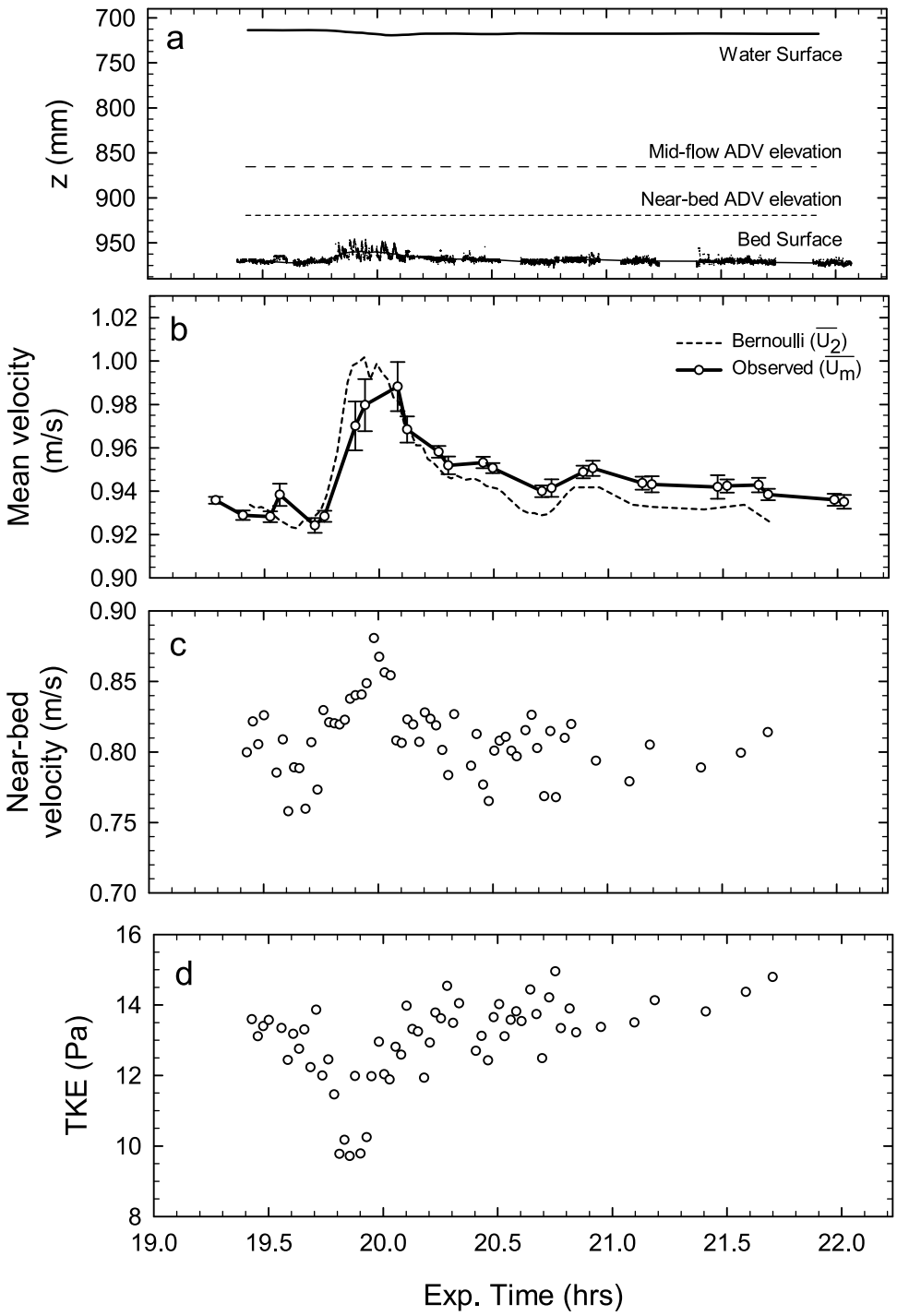

Figure 4. Measured changes in hydraulics and the near-bed flow structure associated with passage of the pulse during run 21c: (a) water and bed surface elevation z and probe elevations (dashed lines), (b) observed ($\overline{U}_m$) and predicted ($\overline{U}_2$) mean velocities, (c) measured near-bed velocities, and (d) near-bed turbulent kinetic energy (TKE). In Figure 4a, z is relative to the instrument cart railways above the flume. Error bar range in Figure 4b represents 1 standard deviation and is intended to represent variability. The fractional error in the observed velocities in Figures 4b and 4c are <0.2% and <0.4%, respectively, indicating that these quantities are known almost exactly.

the sensor array because $\overline{U}_m$ increased as the crests of low-amplitude waves passed and decreased as troughs passed.

[24] Overall, $\overline{U}_2$ mirrors $\overline{U}_m$ (Figure 4b). During pulse passage, $\overline{U}_2$ exceeds $\overline{U}_m$, probably because the low-amplitude waves of the pulse offered some form of resistance to flow not considered in the $\overline{U}_2$ calculation. However, after the topographic expression of the pulse had left the flume, $\overline{U}_2$ was less than $\overline{U}_m$, suggesting that the bed was hydraulically smoother than before the pulse was intro-

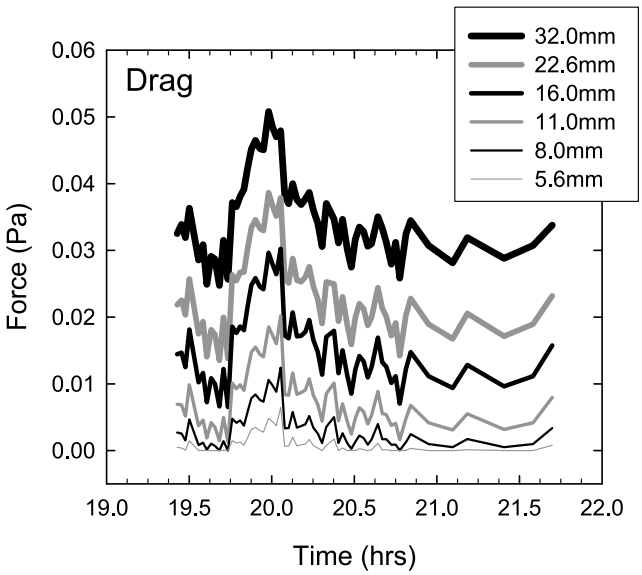

Figure 5. Drag forces acting on a 32 mm particle with various projections above the mean bed elevation calculated from velocity data collected during run 21c. Projections of 4, 2.8, and 2 mm are not plotted because they are below the plane of zero velocity and have drag force values of zero.

duced. If this is the case, the effect should be reflected in the near-bed fluid velocities and turbulence production.

[25] Figures 4c and 4d plot the changes in near-bed velocity and turbulent kinetic energy as the pulse passed beneath the velocity probe. Turbulent kinetic energy is calculated as

$$\mathrm{TKE} = \frac{1}{2}\rho_w\left(\overline{u'^2} + \overline{v'^2} + \overline{w'^2}\right), \tag{3}$$

where the prime superscript indicates a fluctuation in the components of velocity (streamwise u, cross-stream v, and vertical w) in Cartesian space. TKE represents the energy extracted from the mean flow by the motion of turbulent eddies [*Kline et al.*, 1967; *Bradshaw*, 1971] and its production in open channel flow occurs at the boundary where roughness elements generate turbulent eddies.

[26] In the absence of a smoothing effect, as the bed rises toward the height of the velocity sensor, the fluid velocity should decline and the level of turbulence should increase. The exact opposite pattern is observed. As the pulse migrated beneath the instrument array, there was a distinct acceleration in near-bed velocities (Figure 4c), and after the pulse had passed the instrument array, there was a subtle decline in near-bed velocities of ~50 mm/s as the fine pulse particles were exhausted from the bed surface. The level of turbulence declined as the main body of the pulse passed the instruments (Figure 4d). This occurred even though low-amplitude bed waves were present, which would be expected to increase the production of turbulence at the bed. There is too much scatter in TKE to determine if turbulence levels remained low after pulse passage, but it appears that the pulse reduced the scale of turbulence being generated at the boundary.

3.4. Pulse Effects on Forces Acting on Sediment Particles

[27] In order to examine the effects of fluid accelerations due to bed smoothing, we can calculate the drag force responsible for entraining the largest particles in the bed. We focus on the drag force for two reasons. First, it is widely held that drag forces dominate over lift forces in flows just above the entrainment threshold [e.g., *Shields*, 1936]. Second, there is less agreement about the theory used to estimate lift forces from streamwise velocities. Recent work by *Schmeeckle et al.* [2007] has demonstrated that while the drag force is well correlated with streamwise velocity, as indicated by theory [*Wiberg and Smith*, 1987], lift forces were poorly correlated to fluid velocities. This suggests that the theory for estimating lift forces requires careful examination, which is beyond our present purposes, so we focus on changes in the drag force due to smoothing.

[28] The drag force acting on the particle is $F_d = \frac{1}{2}\rho_w\langle u\rangle^2 C_D A_x$, where the angle brackets indicate an average over the grain cross section, C_D is a drag coefficient normally taken as 0.4, and A_x is the area exposed to the flow in the streamwise direction [*Wiberg and Smith*, 1987]. For simplicity, we can assume that $\langle u\rangle = (u_T + u_B)/2)$, where u_T and u_B are fluid velocities at the top and bottom of the particle, and that $u_B = 0$, so $\langle u\rangle = u_T/2$. Now u_T can be estimated from the measured velocities by assuming that the profile is log linear to the top of the particle and by assuming that $u_T = 0$ if the particle projection is less than the plane of zero velocity (z_0) calculated from the velocity measurements. If we assume that the particles are spherical, A_x can be calculated from geometric arguments for the area of circles and circular segments.

[29] Figure 5 plots the calculated drag forces acting on a 32 mm particle with nine different projections (in the sense of *Kirchner et al.* [1990]) above the mean bed elevation ranging from 2 to 32 mm. If a particle has a projection of 32 mm, it is sitting on top of the fine gravel pulse material. If the projection is 2 mm, only the surface of the particle is exposed, and it lies below z_0, the plane of zero velocity. Indeed, all projections $\leq$4 mm are below z_0, so the force acting on those particles is zero. Figure 5 demonstrates that as the sediment pulse passed through the channel, the drag forces responsible for grain entrainment increased dramatically, up to 2× for many projections, and that the magnitude of the increase was dependent on the projection. As the pulse material exited the channel, there was a steady decline in the drag force acting on large particles toward the values initially observed for the bed.

[30] The data presented in Figures 4 and 5 indicate a dominant mechanism responsible for the entrainment of the coarse surface layer by finer gravel in our experiments. Prior to the fine gravel addition, the coarse surface layer of gravel induces high levels of turbulent kinetic energy and reduced local velocities, and the limited finer particles present reside in deep pockets and the lee of the larger stones. Movement of the coarser particles is rare, and once moved, the particles will tend to be stopped by wakes and physical resistance of nearby similar sized rocks. The arrival of significant amounts of fine gravel leads to infilling of the pockets and the lee of larger stones, reduced turbulent kinetic energy, and increased mean flow and, therefore, drag on the exposed larger particles. As a result, the probability of entrainment of

the coarsest particles in the bed material, which were static prior to the pulse, is increased. Because distrainment pockets have been filled by fine particles, the coarsest particles remain in motion.

4. Discussion

[31] The observations presented here show that a fine gravel supply to a much coarser immobile bed dramatically increases bed material transport rates in the channel because the coarse surface layer becomes mobile. Our fluid flow measurements confirm previous hypotheses [*Whiting et al.*, 1988; *Dietrich et al.*, 1989] that infilling the pockets in the coarse surface layer results in damping of the wakes formed in the lee of particles, accelerating the near-bed velocities. *Sambrook-Smith and Nicholas* [2005] made similar observations of the effect of sand additions to a static gravel bed and found that sand content increases near-bed velocities and decreases turbulent kinetic energy and shear stress. However, they hypothesized that the decrease in turbulent kinetic energy and shear stress would decrease gravel transport rates and fine the bed load. While the bed load (pulse and bed material) does become finer, this occurs because of the fine supply that comes from the sediment pulse and transport rates of the coarse bed material surface (excluding pulse material) increased rather than decreased, which coarsened the bed material load. This suggests that while turbulent fluctuations at the bed are damped by the fine pulse, the increase in near-bed velocity may be sufficient to increase coarse particle mobility.

[32] Whether increased near-bed velocity is solely responsible for the increase in mobility is difficult to determine from our data. Partial burial of coarse particles occurs as the concentration of fine gravel on the surface increases. This would logically increase the force necessary to overcome the particle weight. Further, spatial variability in fine gravel coverage leads to spatial variability in the near-bed shear stress, which might also play a role in grain mobility. As such, the increase in near-bed velocity should be thought of as increasing the probability of particle entrainment rather than the sole cause of increased mobility.

[33] The mobilization caused by the introduction of fine gravel pulses influenced the measured sediment flux in three distinct phases. In the first phase, the pulse had entered the channel but did not extend to the end of the flume. Here a carpet of fine grains developed that filled pockets in the coarse surface layer downstream of the topographic expression of the pulse. This carpet of grains gradually covered more of the bed aerially and grew in thickness, filling available pockets in the bed surface. Ultimately, this led to coarse surface layer entrainment. These mobilized coarse particles typically continued to travel downstream to the area of the bed where pulse particles had not yet filled in the surface layer and where they distrained in the available pockets. Only when the carpet had extended to the end of the channel did coarse particles exit the flume along with the pulse material.

[34] In the second phase, the main body of the pulse moved through the channel, and coarse particles were entrained when exposed between the low-amplitude waves formed in the pulse material. These coarse particles traveled over the nearly symmetric waves, sometimes stopping in an available pocket between waves, but usually continued to travel onto the carpet downstream of the topographic expression of the pulse and out of the flume. While these low-amplitude waves were commonly observed in the larger pulse runs described here, it is important to note that they were not an essential component of the mobilization process. We observed that even during very small pulses in other experiments, without enough mass to generate waves, coarse grains were mobilized when a sufficient coverage of fine gravel particles was reached.

[35] In the final phase, after the main body of the pulse had exited the channel, the accelerated near-bed velocity continued to enhance the entrainment rate of particles. But in this phase, the particles rarely exit the flume because of the increasing abundance of distrainment locations. Greatest mobilization of coarse grains out of the flume occurs when the fine gravel carpets the entire length of the flume. There has been systematic study of the probability of entrainment from water-worked sediment in flumes [*Kirchner et al.*, 1990] and the field [*Buffington et al.*, 1992] and work on distrainment processes [*Drake et al.*, 1988]. Our observations suggest that whether particles contribute to measured bed load flux is determined by both the probability of entrainment and the probability of distrainment (as suggested by *Parker et al.* [2003]). Further work is needed to quantify the relative importance of increased near-bed velocity and loss of distrainment sites on increased transport rates.

[36] A wide variety of phenomena are linked to the increased mobilization process when sand is added to gravel material, including the formation and dynamics of bed load sheets [cf. *Iseya and Ikeda*, 1987; *Whiting et al.*, 1988] and increased bed load transport rates (*Ikeda* [1984], *Jackson and Beschta* [1984], and the extensive work by Wilcock cited therein). The results presented here suggest that we should find bed load sheets in sediment mixtures devoid of sand. Indeed, we were able to identify well-defined bed load sheets as we developed the coarse surface layer in experiments that used the same bed material and flows [see *Nelson et al.*, 2009]. Our findings suggest that the empirical analysis by Wilcock and others [*Wilcock*, 1998; *Wilcock and Kenworthy*, 2002; *Wilcock and Crowe*, 2003] that documents a reduction in critical shear stress of gravel with increasing abundance of sand needs to be broadened to account for the general tendency of coarse particles to be mobilized by a critical amount of finer particles. Instead of sand abundance, the essential term is presumably the percent bed coverage by some grain size that is a critical ratio of the coarser bed material. Experimental studies specifically exploring the grain ratio and percent bed coverage for mobilization are needed.

[37] The clear evidence that fine gravel can mobilize coarser gravel suggests an application in gravel augmentation programs. Gravel river beds downstream of dams typically coarsen [*Harvey et al.*, 2005] and become essentially immobile, leading to a reduction in the available salmon spawning and rearing habitat. Gravel augmentation (replacing the sediment supply by dumping gravel into the river) is now common practice and is typically applied with the goal of resurfacing or burying the static coarse bed. An alternative approach may be to use finer sediment to mobilize the static coarse surface layer, creating the poten-

tial to release fine material trapped beneath the surface and temporarily fining the bed. Sand cannot be used to mobilize static gravel beds because of a perceived damaging effect on salmon spawning and rearing habitat. Our results suggest that coarse immobile gravel downstream of dams can be mobilized by adding sediment pulses composed of the fine gravel tail of the channel bed surface grain size distribution.

5. Conclusions

[38] Adding sand to gravel beds is known to greatly increase gravel mobility and flux. Here we demonstrate that additions of fine gravel to a coarser gravel bed can also increase the flux of the coarser gravel bed material. Our experiments demonstrate that finer gravel will fill the interstitial pockets in a coarse surface layer, mobilizing an otherwise static bed. Fine gravel pulses cause systematic changes in channel hydraulics that promote the mobilization process. As fine pulses pass over a gravel bed, the water surface drops, mean flow and near-bed velocities accelerate, and turbulent kinetic energy declines, indicating a decline in the turbulent fluctuations at the bed. However, the increase in coarse particle movement suggests that the increase in drag caused by the accelerated flow may be sufficient to overcome the decline in turbulent fluctuations. Our findings suggest that expressions for the influence of sand on gravel beds need to be generalized as a critical ratio of the finer sediment to the coarser bed material.

[39] **Acknowledgments.** This work was supported by the CALFED Science Program (contract ERP-02D-P55). The instrumentation described herein was designed and constructed by Jim Mullin and Chris Ellis at the National Center for Earth Surface (NCED). Additional support for the equipment, experiments, and analysis was provided by NCED. Technical support for the project was kindly provided by Stuart Foster (UC Berkeley), John Potter (UC Berkeley), and Kurt Yaeger (SFSU). The experimental design benefited from the initial input of the project's scientific advisory panel, which included Peter Wilcock (Johns Hopkins University), Gary Parker (University of Illinois), Tom Lisle (U.S. Forest Service), Scott McBain (McBain and Trush, Inc.), and Kris Vyverberg (California Department of Fish and Game).

References

Bradshaw, P. (1971), *An Introduction to Turbulence and Its Measurement*, Pergamon, Toronto.

Buffington, J. M., W. E. Dietrich, and J. W. Kirchner (1992), Friction angle measurements on a naturally formed gravel streambed: Implications for critical boundary shear stress, *Water Resour. Res.*, *28*, 411–425, doi:10.1029/91WR02529.

Curran, J. C., and P. R. Wilcock (2005), The effect of sand supply on transport rates in a gravel-bed channel, *J. Hydraul. Eng.*, *131*, 961–967, doi:10.1061/(ASCE)0733-9429(2005)131:11(961).

Dietrich, W. E., J. W. Kirchner, H. Ikeda, and F. Iseya (1989), Sediment supply and the development of the coarse surface layer in gravel-bedded rivers, *Nature*, *340*, 215–217, doi:10.1038/340215a0.

Drake, T. G., R. L. Shreve, W. E. Dietrich, P. J. Whiting, and L. B. Leopold (1988), Bedload transport of fine gravel observed by motion-picture photography, *J. Fluid Mech.*, *192*, 193–217, doi:10.1017/S0022112088001831.

Harvey, B., S. McBain, D. Reiser, L. Rempel, L. S. Sklar, and R. Lave (2005), Key uncertainties in gravel augmentation: Geomorphological and biological research needs for effective river restoration, report, 99 pp., CALFED Sci. Program, Sacramento, Calif.

Ikeda, H. (1984), Flume experiments on the superior mobility of sediment mixtures, *Ann. Rep. Inst. Geosci. 10*, pp. 53–56, Univ. of Tsukuba, Tsukuba, Japan.

Iseya, F., and H. Ikeda (1987), Pulsations in bedload transport rates induced by a longitudinal sediment sorting: A flume study using sand and gravel mixtures, *Geogr. Ann., Ser. A, Phys. Geogr.*, *69*, 15–27, doi:10.2307/521363.

Jackson, W. L., and R. L. Beschta (1984), Influences of increased sand delivery on the morphology of sand and gravel channels, *J. Am. Water Resour. Assoc.*, *20*(4), 527–533, doi:10.1111/j.1752-1688.1984.tb02835.x.

Kellerhals, R., and D. I. Bray (1971), Sampling procedures for coarse fluvial sediments, *J. Hydraul. Div. Am. Soc. Civ. Eng.*, *97*(HY8), 1165–1180.

Kirchner, J. W., W. E. Dietrich, F. Iseya, and H. Ikeda (1990), The variability of critical shear stress, friction angle, and grain protrusion in water-worked sediments, *Sedimentology*, *37*, 647–672, doi:10.1111/j.1365-3091.1990.tb00627.x.

Kline, S. J. W., W. C. Reynolds, F. A. Schraub, and P. W. Rundstadler (1967), The structure of turbulent boundary layers, *J. Fluid Mech.*, *30*, 741–773, doi:10.1017/S0022112067001740.

Nelson, P. A., J. G. Venditti, W. E. Dietrich, J. W. Kirchner, H. Ikeda, F. Iseya, and L. S. Sklar (2009), Response of bed surface patchiness to reductions in sediment supply, *J. Geophys. Res.*, *114*, F02005, doi:10.1029/2008JF001144.

Parker, G. (2007), Transport of gravel and sediment mixtures, in *Sedimentation Engineering: Theories, Measurements, Modeling and Practice*, *ASCE Manual Rep. Eng. Practice*, vol. 110, edited by M. H. Garcia, chap. 3, pp. 165–264, Am. Soc. of Civ. Eng., Reston, Va.

Parker, G. (2009), *1D Sediment Transport Morphodynamics With Applications to Rivers and Turbidity Currents* [electronic], Civ. and Environ. Eng., Univ. of Ill. at Urbana-Champaign, Urbana. (Available at http://vtchl.uiuc.edu/people/parkerg/morphodynamics_e-book.htm)

Parker, G., and P. C. Klingeman (1982), On why gravel bed streams are paved, *Water Resour. Res.*, *18*, 1409–1423, doi:10.1029/WR018i005p01409.

Parker, G., G. Seminara, and L. Solari (2003), Bed load at low Shields stress on arbitrarily sloping beds: Alternative entrainment formulation, *Water Resour. Res.*, *39*(7), 1183, doi:10.1029/2001WR001253.

Sambrook Smith, G. H., and A. P. Nicholas (2005), Effect on flow structure of sand deposition on a gravel bed: Results from a two-dimensional flume experiment, *Water Resour. Res.*, *41*, W10405, doi:10.1029/2004WR003817.

Schmeeckle, M. W., J. M. Nelson, and R. L. Shreve (2007), Forces on stationary particles in near-bed turbulent flows, *J. Geophys. Res.*, *112*, F02003, doi:10.1029/2006JF000536.

Seminara, G., M. Colombini, and G. Parker (1996), Nearly pure sorting waves and formation of bedload sheets, *J. Fluid Mech.*, *312*, 253–278, doi:10.1017/S0022112096001991.

Shields, A. (1936), Anwendung der Aehnlichkeitsmechanik und der Turbulenzforschung auf die Geschiebebewegung, *Mitt. 26*, Preuss. Versuchsanst. fuer Wasserbau und Schiffbau, Berlin. (English translation, W. P. Ott and J. C. van Uchelen, *Publ. 167*, Hydrodyn. Lab., Calif. Inst. of Technol., Pasadena, 1950.)

Sklar, L. S., J. Fadde, J. G. Venditti, P. Nelson, M. A. Wydzga, Y. Cui, and W. E. Dietrich (2009), Translation and dispersion of sediment pulses in flume experiments simulating gravel augmentation below dams, *Water Resour. Res.*, *45*, W08439, doi:10.1029/2008WR007346.

Venditti, J. G., M. Church, and S. J. Bennett (2005), Morphodynamics of small-scale superimposed sand waves over migrating dune bed forms, *Water Resour. Res.*, *41*, W10423, doi:10.1029/2004WR003461.

Venditti, J. G., W. E. Dietrich, P. A. Nelson, M. A. Wydzga, J. Fadde, and L. Sklar (2010), Effect of sediment pulse grain size on sediment transport rates and bed mobility in gravel bed rivers, *J. Geophys. Res.*, doi:10.1029/2009JF001418, in press.

Whiting, P. J., W. E. Dietrich, L. B. Leopold, T. G. Drake, and R. L. Shreve (1988), Bedload sheets in heterogeneous sediment, *Geology*, *16*, 105–108, doi:10.1130/0091-7613(1988)016<0105:BSIHS>2.3.CO;2.

Wiberg, P. L., and J. D. Smith (1987), Calculations of the critical shear stress for motion of uniform and heterogeneous sediments, *Water Resour. Res.*, *23*, 1471–1480, doi:10.1029/WR023i008p01471.

Wilcock, P. R. (1998), Two-fraction model of initial sediment motion in gravel-bed rivers, *Science*, *280*, 410–412, doi:10.1126/science.280.5362.410.

Wilcock, P. R., and J. C. Crowe (2003), A surface-based transport model for sand and gravel, *J. Hydraul. Eng.*, *129*(2), 120–128, doi:10.1061/(ASCE)0733-9429(2003)129:2(120).

Wilcock, P. R., and S. T. Kenworthy (2002), A two-fraction model for the transport of sand/gravel mixtures, *Water Resour. Res.*, *38*(10), 1194, doi:10.1029/2001WR000684.

Wilcock, P. R., and B. W. McArdell (1993), Surface-based fractional transport rates: Mobilization threshold and partial transport of a sand-gravel sediment, *Water Resour. Res.*, *29*, 1297–1312, doi:10.1029/92WR02748.

Wilcock, P. R., and B. W. McArdell (1997), Partial transport of a sand/gravel sediment, *Water Resour. Res.*, *33*, 235–245, doi:10.1029/96WR02672.

Wilcock, P. R., S. T. Kenworthy, and J. C. Crowe (2001), Experimental study of the transport of mixed sand and gravel, *Water Resour. Res.*, *37*, 3349–3358, doi:10.1029/2001WR000683.

Williams, G. P. (1970), Flume width and water depth effects in sediment transport experiments, *U.S. Geol. Surv. Prof. Pap.*, *562-H*, 37 pp.

W. E. Dietrich and P. A. Nelson, Department of Earth and Planetary Science, University of California, Berkeley, CA 94720, USA.

J. Fadde and L. Sklar, Department of Geosciences, San Francisco State University, San Francisco, CA 94132, USA.

J. G. Venditti, Department of Geography, Simon Fraser University, Burnaby, BC V5A 1S6, Canada.

M. A. Wydzga, Department of Earth Science, University of California, Santa Barbara, CA 93106, USA.